Supporting Information

Shadow Enabled Non-Invasive Probe for Multi-Feature Intelligent Liquid Surveillance System

*Lizhen Lian [a, b, c], Qian Zhang [a, *], Wenbo Li [b], Bin Wang [c, *], and Qijie Liang [b, *]*

[a]School of Materials, Shenzhen Campus of Sun Yat-sen University, No. 66, Gongchang Road, Guangming District, Shenzhen 518107, China

[b]Songshan Lake Materials Laboratory, Songshan Lake Mat Lab, Dongguan 523808, China

[c]School of Physics and Materials Science, Guangzhou University, No.230, University Town Waihuan West Road, Guangzhou 510006, China

* Corresponding authors.

E-mail addresses: zhangqian6@mail.sysu.edu.cn (Q. Zhang), binwang@gzhu.edu.cn (B. Wang), liangqijie@sslab.org.cn (Q. Liang).

Contents

Effect of Au film thickness on SP performance

It is important to choose the most effective thickness of the Au film for the Au/n-Si system. As shown in Figure S1a, the I_{sc} generated by the SP with 15nm, 45 nm, and 90 nm Au films are 508 μA, 320 μA, and 88μA, respectively. In Figure S1b, the V_{oc} generated by the SP with 5 nm, 45 nm, and 90 nm Au films are 420 mV, 295 mV, and 182 mV, respectively. In a word, the I_{sc} and V_{oc} generated by the SP with a 15 nm Au film are much higher than those generated by the systems with 45 nm and 90 nm Au films. Because n-Si is the main source of photo-generated carriers, the thickness of the Au film affects the light intensity reaching the surface of Si. This observation can be attributed to the decrease in transparency as the thickness of the Au film increases. Therefore, a 15 nm Au film is used to fabricate the SP.

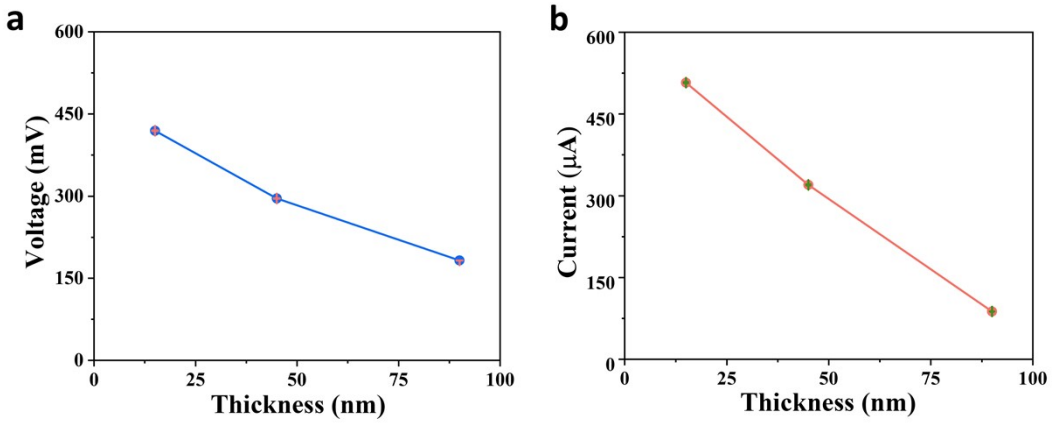

Figure S1. Comparison of the I_{sc} (a) and the V_{oc} (b) generated with different Au film thicknesses (15 nm, 45 nm, 90 nm).

Note S1. The KPFM testing of the SP

To enhance the demonstration of the working principle of the device, measurements of the work function on the surface of Au/n-Si were conducted. This was achieved by utilizing a Pt/Ir tip (5.5 eV) in conjunction with a Kelvin probe force microscope (KPFM) under two distinct conditions, simulating both illuminated and dark environments resembling sunlight. The calculation formula for the work function (W_{surface}) before and after illumination is as follows:

$$W_{surface} = W - CPD \times e^{-} \tag{S1}$$

CPD stands for Contact Potential Difference, and W_{tip} refers to the work function of the Pt/Ir tip used for scanning in KPFM. Under illumination, the work function of the Au/n-Si surface changes from 5.29 eV to 5.45 eV.

Note S2. The proposed equivalent model of the SP for liquid detection from characteristics of liquid shadows

When half of the SP area is covered by the shadow and the other half is illuminated, electrons in the illuminated region are knocked free by photons. The Schottky barrier potential under illumination φ_b* is determined by the equation S2, [s1, s2]

$$\varphi_b{}^* = \varphi_b - nhv = \varphi_b - \frac{nhc}{\lambda} \tag{S2}$$

where h is Planck constant, ν is the frequency, c is the speed of light, n is the number of photons, and λ is the wavelength. Therefore, there are three main factors being proposed to influence the output voltage. The first factor is the light wavelength variations ($\Delta\lambda$) between the illuminated and shaded regions of the SP. When half of the SP area is in absolutely shadow (covered by black paper in this work), the photons with different λ induces different responses to SP. On the contrary, when half of the SP area is in illumination while the other half is in liquid shadows, the output voltage of the SP changes due to the $\Delta\lambda$.

As shown in equation S3, the number of photons is related to light intensity (P), the area of the illumination area (A), and the illumination time (t).

$$P = \frac{nhv}{At} \tag{S3}$$

The illumination time of the illuminated and shadow region is equal. So the second and third factors influencing output voltage of the SP are illumination contrast (ΔP) between the illuminated and shaded regions of the SP and the shadow area change (ΔA).

Note S3: The detailed calculation process about the unit price of SP

In determining the fabrication cost of scanning probes (SP), we consider two key materials: n-Si and Au. The cost breakdown is as follows:

The price of n-Si is \$ 0.07/cm^2.

The size of the SP is 4 cm × 2 cm.

The volume of the Au film:

$$4\ cm \times 2\ cm \times 15\ nm = 0.00012\ cm^3$$

Cost of n-Si:

$$\$\ 0.07/cm^2 \times (4\ cm \times 2\ cm) = \$\ 0.07/cm^2 \times 8\ cm^2 = \$\ 0.56$$

Cost of Au film (calculated based on the current gold price).:

$$0.00012\ cm^3 \times 19.32\ g/cm^3 \times \$\ 60.3/g = \$\ 0.14$$

Cost of each SP:

$$\$\ 0.56 + \$\ 0.14 = \$\ 0.7$$

Therefore, the estimated manufacturing cost of each SP is approximately \$ 0.7/cm^2, considering both the n-Si material and the gold film expenses.

The robustness of SP in cycling testing.

To assess the stability of the SP, a repeated light-switching test was conducted on the device at 0.1 sun with a 50% shadow area. During more than 1000 cycles, the I_{sc} and V_{oc} states of the SP were recorded. Figure S2 shows detailed output curve of the SP under pulsed illumination during 100 cycles.

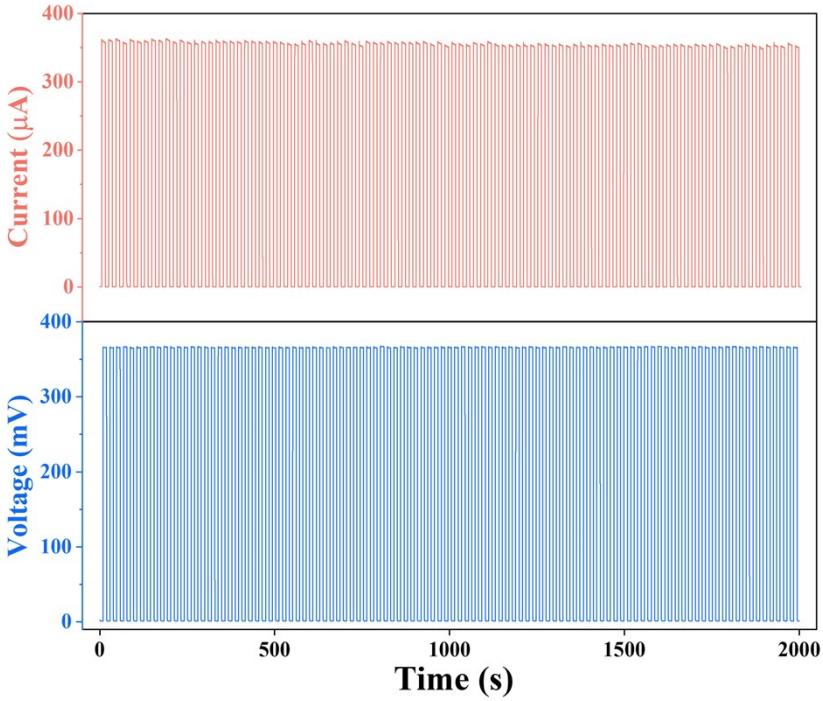

Figure S2. Detailed half-shadow output curve of the SP under pulsed illumination (0.1 sun) during 100 cycles.

Detailed data of SP for liquid color detection

Under the same light intensity, 8 liquids with different colors were placed in front of SP as shelter. Then, use a multi-meter to directly measure the output of the SP. As shown in Figure S3, the output of SP shows a significant difference. Because the different colors of the liquid will selectively absorb the corresponding band of light. Due to differences in test light sources and circuit loads, the V_{oc} data of the multi-meter is not the same as that of the ILSS. However, compared to orange, red, and blue liquids, the output of green liquids was significantly higher. This is consistent with the ILSS detection results.

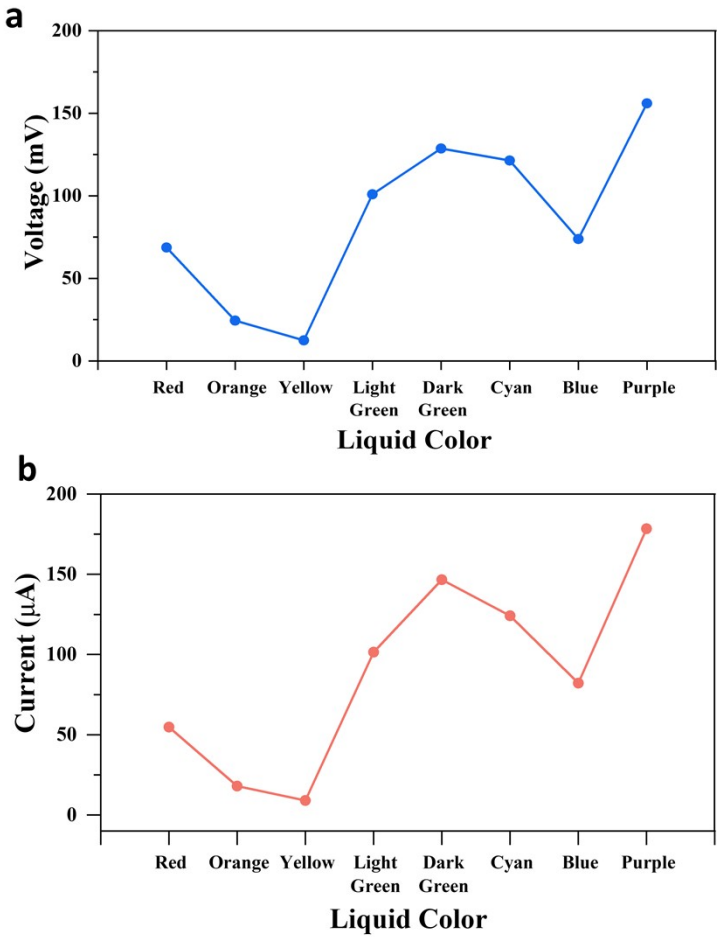

Figure S3. Using a multi-meter measurement to compare (a) V_{oc} (b) I_{sc} of the SP through different colors of liquids.

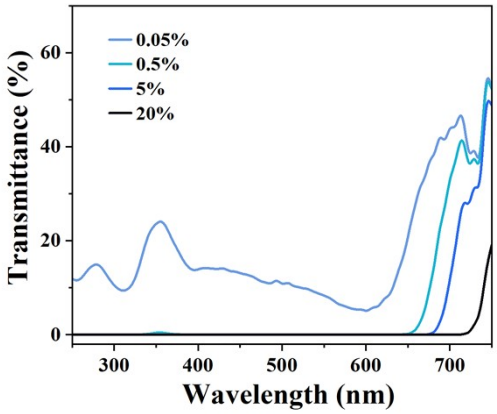

Figure S4. Transmittance of 4 different concentrations (0.05%, 0.5%, 5%, 20%) of liquids using UV-vis.

Detailed data for SP for liquid concentration detection.

Similarly, the output of SP is measured directly with a multi-meter when only the concentration of the liquid is changed. As shown in Figure S4, the output changes caused by 9 different concentrations of black liquid are compared. As the concentration increases, the V_{oc} and I_{sc} of SP continue to increase. The increase in concentration results in an increase in illumination and shadow contrast on the SP surface.

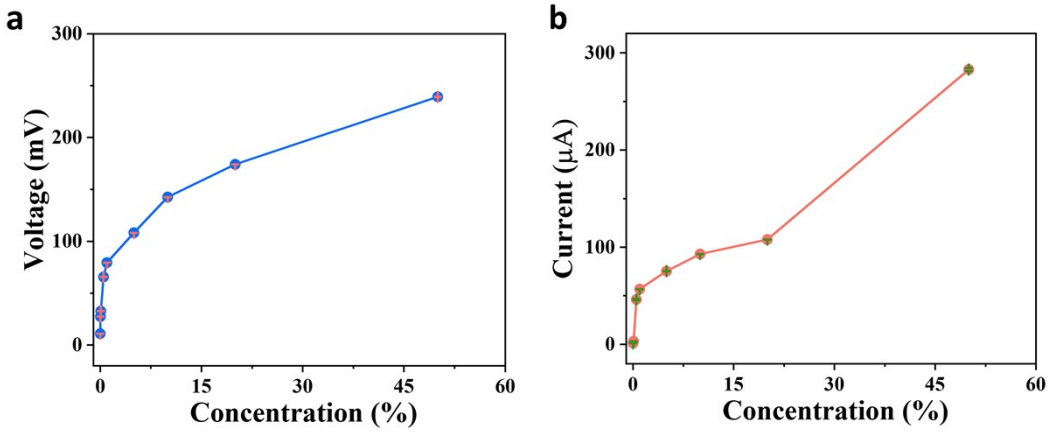

Figure S5. Using a multi-meter measurement, compare (a) V_{oc} (b) I_{sc} of the shadow effect device through different concentrations of liquid.

Detailed data for 2-channel SP for liquid level detections

To further verify the reliability of the 2-SPs array, use a multi-meter to measure the output separately when the liquid level changes from 0 to 1. The SP 1 is located at the bottom, as shown in Figure S5a and S5b, and the V_{oc} and I_{sc} are higher at 1/2 level than at other levels. The SP 2 is located higher, which is at 1/2 the height of SP 1. As shown in Figure S5c and S5d, when the liquid level is below half, there is almost no significant change in the output V_{oc} and I_{sc} of the SP 2. However, when the liquid level reaches 1, the V_{oc} and I_{sc} of the SP 2 peak. By combining the output of the two channels, the liquid level can be easily determined.

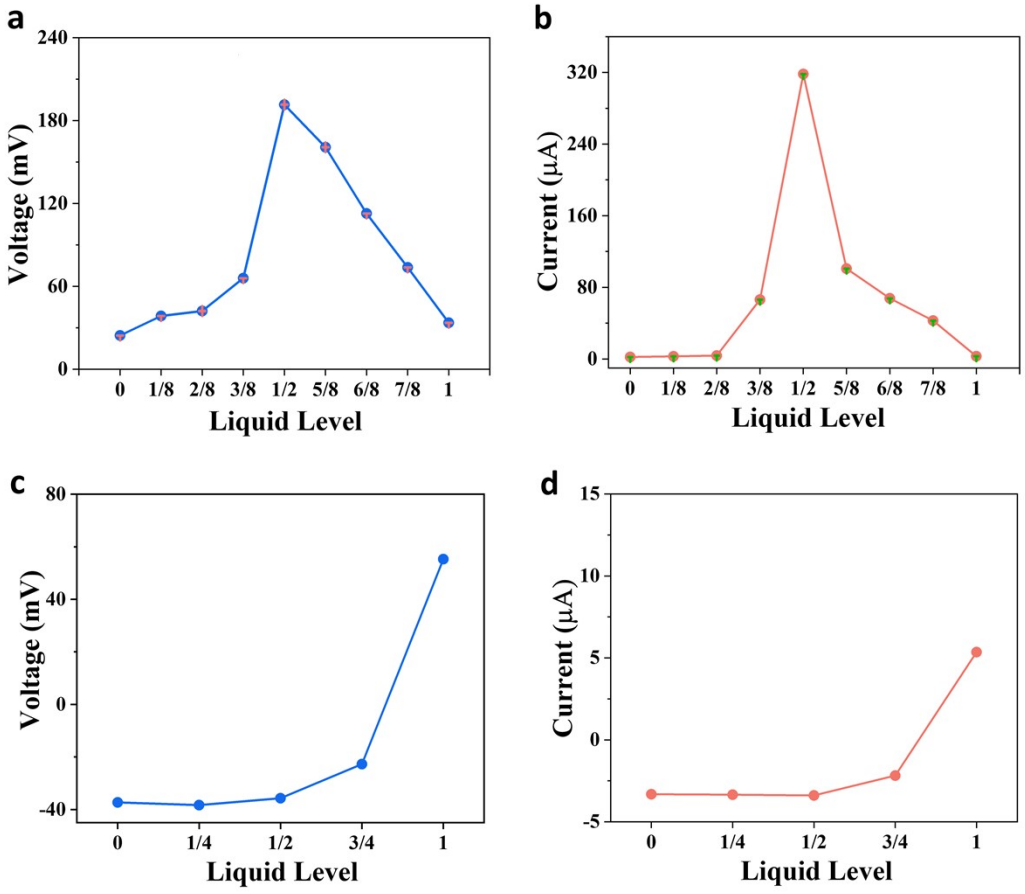

Figure S6. Output of the dual-channel device for detecting different liquid levels using a multi-meter (a) V_{oc} (b) I_{sc} for channel SP 1; (c) V_{oc} (d) I_{sc} for SP 2.

Table S1. The detailed parameters of the 1D-CNN DL architecture.

No	Layer	No. of Filters	Kernel / Pool Size	Stride	Input Size	Output Size	Padding
1	Convolution 1	32	5	1	(None, 200,2)	(None, 200,16)	Same
2	Max-pooling 1		2	2	(None, 200,16)	(None, 100,16)	Same
3	Convolution 2	64	5	1	(None, 100,16)	(None, 100,64)	Same
4	Max-pooling 2		2	2	(None, 100,64)	(None, 50,64)	Same
5	Convolution 3	128	5	2	(None, 50,64)	(None, 25,128)	Same
6	Max-pooling 3		2	2	(None, 25,128)	(None, 12,128)	Same
7	Convolution 4				(None, 12,128)	(None, 12,512)	
8	Max-pooling 4				(None, 12,512)	(None, 6,512)	
9	Flatten				(None, 6,512)	(None, 3072)	
10	Dense (10)				(None, 3072)	(None, 10)	

Table S2. Characteristics of 10 different liquids in the dataset.

Sample number	Color	Concentration	Liquid level
1	Red	1%	1/6
2	Blue	1%	1/3
3	Green	1%	1/2
4	Red	5%	1/2
5	Green	5%	1/6
6	Blue	3%	5/6
7	Orange	5%	5/6
8	Yellow	2%	2/3
9	Purple	2%	2/3
10	Black	10%	1

References

(S1) Z. Sun and Y. Fang, *Sci. Rep*., 2021, **11**, 338.

(S2) Z. Li, W. Ran, Y. Yan, L. Li, Z. Lou and G. Shen, *InfoMat*, 2022, **4**, e12261.